Journal of Progressive Research in Mathematics
Vol 17,1 - 2020 — E-ISSN: 2395-0218
http://www.scitecresearch.com/journals/index.php/jprm

Homology Theory on Causal Random Groups

M.M. Khoshyaran[1]

[1] Economics Traffic Clinic, ETC, Paris, France.

Received: November 12, 2020; Accepted: December 1, 2020; Published: December 15, 2020

Abstract

The objective of this paper is to analyze a new approach to homology theory that deals with Causal Random Groups, (CRG). It is shown that the evolution of (CRG) can be tracked down as these groups stay within the general random groups category. Random groups are algebraic groups that are not systematically the result of interaction of several random sub algebraic groups. Therefore, in general random groups are unstable. Evolution is change from a known state that can be traced back to that state. If change can not be traced back to its' initial state, then this change results in a shift to an unknown zone. Change within the unknown zone is designated as evolution in complex domain. The method of tracing in complex domain is outlined and analyzed. It is proven that all change in complex domain stays within the limits defined by causal random algebraic groups. Eventually, (CRG) can reach stability (equilibrium) when repeated change in the complex domain finally leads to emergence from the unknown zone onto a state in real space. A rectangular slab is used to represent causal elements. The relationship between causal elements is depicted as a network of links and paths on each face of the slab, and the space between any two opposing faces. This space is refereed to as internal networks. Hyperplanes and hyperplane pencils are used to cut segments on the networks on the faces, and geodesics are used to explore zones in the internal networks. Zones on any face of the slab are considered to be in the real space, and zones in the internal network are in the complex space. If the boundary points of the zones are on tangent bundles to hyperplane pencils, then these points are non-singular, otherwise the zone contains singularity. Then the focus is shifted onto the internal networks, similar search is done this time with geodesics. Path on non-singular points connect stable, irreducible, cuasal elements, and any sub-group of (CRG) built on these points is complete and optimal.

Keywords

Homology theory; Causal Random Groups; causality; hyperplanes; hyperplane pencils; causal chains; neighboring points; transition homology; parallax causal points; complex regions; geodesics; cones; vertices of cones; equilibrium state; stable; complete.

ACM

81T45,18D05.

1. Introduction

The objective of this paper is to introduce and analyze a new approach to homology theory that deals with Causal Random Groups, (CRG), denoted by $(G(X))$ [1], where (X) is the space of causal elements. CRG are those groups that do not obey certain rules regularly, but still stay in the same general random group category. This means that random groups change their size due to causality external to the general rules of the random groups. Therefore, if a random algebraic group (G) is of size $(n \geq 0)$, its size can vary from (n) to $(n - s; s \leq n)$ without any change in the nature of the random algebraic group. The size of (CRG) is the number of causal elements that build the structure of (CRG). A rectangular slab is used to represent causal elements. Each node of the rectangular slab represents a causal element. Each rectangular slab contains (8) causal elements. To include more causal elements, it suffices to attach more rectangular slabs to each other. Each rectangular slab contains (6) faces. There exists a space between any two opposing faces. The faces of the rectangular slab are considered to exist in the real space, $(\Re^n)$. The space between any two faces exists in complex space,$(\mathbf{Z}^n)$. The relationship between causal elements is depicted as a network of links and paths on each face of the slab, and in the space between any two opposing faces. On each face of the slab, it is possible to connect causal elements through alternate paths. Each path consists of a collection of links. The origins and destinations of each path are causal elements. The intermediate points are called causal chains. These points exist due to the complexity of causal elements. Each causal element has several dimensions. A dimension represents a characteristic of a causal element. Each dimension has is considered to have several degrees of intensities for each dimension. The level of the complexity of a causal element depends on the existing knowledge of the causal element. The higher the level of complexity, the larger are the number of causal chains on the paths. These paths are considered to be very important since outside of these paths there is no information about the relationship among causal elements. Path on non-singular points connect stable, irreducible, causal elements, and any sub-group of (CRG) built on these points is complete and optimal.

The space between any two opposing faces is refereed to as internal networks. The networks inside the slab consists of alternate paths. Each path is a collection of links. Each path is from an origin to a destination on a face of the rectangular slab. The origins and destinations are causal element nodes on the faces of the rectangular slab. The intermediate points in the internal networks are Parallax causal elements. Parallax causal elements are those causal elements that are not in the list of causal elements since there is a gap between parallax elements and the direct causal elements. Parallax causal elements are the origin and destination points of the links. Any point on a link between Parallax causal elements are called the neighboring points. The neighboring points play an important role in the search process for optimal sub-groups of (CRG). Hyperplanes and hyperplane pencils are used to cut segments on the networks on the faces of the slab. In the internal networks, hyperplane pencils are transformed to the dynamics of internal forces. These tools are used in the search process for stable, and irreducible causal elements. The outline of the search process is as follows: on the faces of the slab, a search consists of cutting a zone of the network using hyperplanes and hyperplane pencils. Zones on any face of the slab are considered to be in the real space. Each zone on a face of a rectangular slab, is considered to be the base of a cone cut out by hyperplane pencils and the dual hyperplane pencils outline a dual zone that is considered to be the vertex of this cone. The cone transforms into a cylinder with all parallel hyperplane pencils that are of equal lengths, if the boundary points of the zones are on tangent bundles to hyperplane pencils, then these points are non-singular, otherwise the zone contains singularity. When singularity,then the focus is shifted onto the internal networks, similar search is done this time with geodesics. Zones in the internal network are in the complex space, are found using geodesics in the same way as in the real space. Thus the base of a cone is in the real space, and is the dual zone. The vertex of the cone is in the complex space in the internal networks in the complex space. In the same way, when the points on the boundary of the vertex are non-singular, i.e. possess tangent bundles to geodesics at boundary points, then the cone transforms into a cylinder.

Theorem 1. *If the hyperplane pencils that cut a segment (W) on a face of a rectangular slab, cut points that possess tangents on the boundary of $(\beta(W))$, and the dual region (W') with dual hyperplane pencils,*

and dual tangent bundles that form a cylinder, then the hyperplane pencils are parallel to each other and are all of same lengths.

Proof. The points on the boundary $(\beta(W))$, possess tangent bundles at hyperplane pencils, therefore, these boundary points are non-singular points. Let $(y_{c_a}^{(i)|j}; i = 1, \cdots, I; c_a = 1, \cdots, C_a)$, where (i) is the dimension of each boundary point, be on the boundary of $(\beta(W))$. Let the space of dimensions (I) be a space with one degree of freedom. One degree of freedom of this space gives at most one dimension. Let $(T^{(i-1)}_{y_{c_a}^{(i)|j}})$, represent tangent bundles orthogonal to hyperplane pencils at boundary points, $(y_{c_a}^{(i)|j})$. Let $(\Gamma^{(i)})$ represent hyperplane pencils. Given, the condition of one degree of freedom for dimension (i), the following homeomorphism exists, $(T^{(i-1)} \times \Gamma^{(i)} \to y_{c_a}^{(i)|j})$. Given that any dual segment, (W') is a homeomorphism of (W), then the following homeomorphism exists, $(T'^{(q-s-r)} \times \Gamma'^{(q-s)} \to y_{c_a}^{\prime(i)|j}; (i-1) \leq q \leq I; i = 1, \cdots, (I-1); s, r \leq 0)$, where $(y_{c_a}^{\prime(i)|j})$ are the dual boundary points of $(y_{c_a}^{(i)|j})$, and where homeomorphisms of types $(T^{(i-1)} \times (I) \to T'^{(q-s-r)})$, and $(\Gamma^{(i)} \times (I) \to \Gamma'^{(q-s)})$ exist, and $((T^{(i-1)} \times \Gamma^{(i)}) \to (T'^{(q-s-r)} \times \Gamma'^{(q-s)}))$ is a homeomorphism of $(y_{c_a}^{(i)|j} \to y_{c_a}^{\prime(i)|j})$. Given that the dual dimension space (I') is the dual of dimension space (I), then all hyperplane pencils, and their dual are of equal lengths.

□

The new homology theory is an approach that allows for transition hyperplane pencils (fiber bundles) in the complex domain,[2] without any loss of the characteristics of random algebraic groups. Transition vertices are means to finding the optimal fiber bundles for each random algebraic group, [3]. The optimal fiber bundle is the one for which the vertex contains all non-singular points, and it is not possible to find a neighborhood (ϵ) of any vertex (W) that contains a singular point. The optimal fiber bundles to hyperplane pencils in real space, or geodesics, in complex space, are the ones that all pencils are parallel, (normal tangents) and of the same size.

The advantage of this new approach in homology is that it makes it possible to follow the evolution of such random algebraic groups towards stability (equilibrium), and completeness. This approach to random algebraic groups, has a potential to replace standard optimization methods since in this case, stability and completeness are equivalent to optimality.

2 Random groups

As is mentioned in the introduction, random groups are the groups that do not obey certain rules regularly, but still remain member of the same group. The reason for this is that in fact, random groups are formed from elements that constitute causes. Groups formed from these causal elements are effects. To develop random causal groups, (G), it is important to establish a background for causal elements. It is assumed that all causal elements have some features in common. For example can assume that all causal elements are shapes and they all possess specific dimensions. All causal elements are distinct from each other even though they may share some common features. There exists different degrees of commonality among causal elements. This is measured by calculating distances along dimensions. The shorter the distances among dimensions of any (2) causal elements, the more similar they are. Each dimension has several degrees of intensities. The intensities make up regions. For example if food is a causal element, then it possesses dimensions (characteristics) such as weight, color, shape, and taste. Each dimension, let's say weight has many degrees of intensities, from light to heavy. In this example, the region of dimension weight is a set consisting of degrees of heaviness.

It is more appropriate to call random groups, as causal groups. A causal group retains its' characteristics as long as there are existing causes and thus corresponding effects. Variations in the degree of causality allow for fibering in a complex domain. Each causal element is defined by its dimension. To clarify, let's denote the space of all casual elements forming a group by $(X = \{x_{i,j}^k, k = 1, 2, , \cdots, K; i = 1, \cdots, I; j = 1, \cdots, J\})$,$(X \subset \Re^n)$. Let $(X = \{x_{i,j}^k\})$, contain all causal elements of a group denoted by $(x_{i,j}^k)$, where

(k) is the number of causal elements, (i) represents the dimension of each casual element, and (j) is the number of regions of intensities. To make the concept of dimension and intensity clear, an example from the representation field is chosen, [**?**]. To give an example, let's say that there are a total of ($K = 2$) causal elements, say ocean, and food. The dimension for ocean is those characteristics that describe an ocean, such as color, depth, area, underwater landscape, water pressure, wave formation, beaches, weather, water animals, pollution, and energy level, a total of (I=11) possible dimensions. Of course there are many more characteristics if one wants to be exhaustive. For the causal element food, the dimension is the characteristics that conjure up food such as (taste: saline, bitter, sour, sweet), weight, color, ingredients, spices, fat content, and date of expiration, a total of (I=7) dimensions.

Each characteristic possesses various levels of intensities, let's say from (1) to (10), with (1) being the lowest level of intensity, and (10) being the highest intensity. ($j = 1, \cdots, 10$), meaning that the variable (j) representing intensity levels that go from (1) to (10). For example, ($\{x^2_{1,5}\}$), is the causal element food, ($k = 2$),with characteristic being the color of food,($i = 2$), and with intensity level of color equal to (5), ($j = 5$). It is the interaction between each characteristic of a causal element of a (CRG) with it's various levels of intensities, and another causal elements characteristics and intensities that allow for randomness of (CRG). Therefore, it is important to analyze this relationship in depth. Let's take as an example, the causal element food, and the characteristic taste as the sole characteristic, with (4) levels of intensities, (sweetness, bitterness, sour, and salty). The second causal element is ocean with color as it's sole characteristic, with color having (4) levels of intensities (blue, green, gray, turquoise). The (CRG), (sea food) made of the two causal elements (food, ocean) is the result of the relationship between the two causal elements, through the relationship among the characteristics and their intensities. It is important to have a geometrical representation of the causal random group. This way a metric is created that allows for measurement of the relationship, and thus enabling the analysis of the causal random group with respect to the dynamics of change and stability. The aim is to find at which combination of causal elements a random causal group is at equilibrium. Equilibrium means stable. In the example above, the most stable sub-group of (CRG) would be sea food that comes from a blue ocean, and is salty. An stable random causal group is the one that contains all non-singular points. The existence of singularity is an indication of non-stability. An stable random causal group is a sub-group of the random causal group. This sub-group is invariant and thus can be used as a generator of homeomorphic (CRG) with all non-singular points in real space, ($\Re^n$).

The character, taste of the causal element food with (4) levels of intensities (sweet, salty, bitter, sour) is modeled by (Henning), [6], as a tetrahedron, shown in Figure 1. The Henning tetrahedron for one causal element (food), with (4) dimensions (sweetness, bitterness, sour, and salty), and each dimension (circular disks) with (4) levels of intensities, (each disk is divided into 4 slices) is shown in Figure 1a. Geometrical representation modeling in the field of cognitive science is well established. The general representation theory is based on modeling cognitive concepts such as concept formation, semantics, non-monotonic inferences, and inductive reasoning. A tetrahedron in this context represents concept formation. For example, it is the concept of evolution from sweet to sour. Tetrahedron represents inductive reasoning in the sense that it is logical to go from sweet to sour. The advantage of using geometrical figures to represent the interaction of causal elements is that it allows for the use of metrics to calculate the form, and the impact of the relationship among causal elements. In Figure 1, each face of the tetrahedron is a manifold representing the relationship among dimensions of each causal element and their (4) intensity levels. A (CRG) is formed when causal elements are related. In this example, a (CRG) is formed as an emergence of a phenomenon, (sea food) which is an interaction between the (2) basic causes, (ocean, and food), that creates the effect or (CRG) which is (sea food). Taking the example of (Henning), as a model, it is possible to show this relationship for a causal element space, ($X = \{x^k_{i,j}, k = 1, 2; i = 1, 2, 3, 4; j = 1, 2, 3, 4\}$), with (2) causal elements, having each (4) dimensions or characteristics, and for each dimension (4) levels of intensities, as a tetrahedron, shown in Figure 2. Each vertex of the tetrahedron represents a causal element. Each dimension is represented by a circular disk divided into slices that represent intensities of that dimension. In the example of Figure 2, each causal element has (4) dimensions, therefore, there are (4) circular disks each divided into slices that represent intensities. The lines of tetrahedron represent relationships between causal elements. Therefore

each face of the tetrahedron is a manifold. There exists a line between each dimension and each intensity of causal elements. Manifolds made of lines that connect each dimension and its' intensities to another dimension and its' intensities. For the purpose of demonstration and for avoiding clutter, only few lines are outlined.

In the context of this paper, given that there usually are a large number of causal elements that can be considered, it is preferable to adopt a rectangular slab as a geographical representation, shown in Figure 3. Another reason for choosing a rectangular slab is that it allows for better visualization of the positions of causal elements, specially when there are various degrees of similarities among causal elements. For example, those causal elements that are highly similar, are positioned closer together on a rectangular slab, and those causal elements that have either low or negligible similarities are placed farther away on the rectangular slab. Each rectangular slab allows for (8) causal elements. Each causal element has it's respective dimensions or characteristics, and each characteristic has degrees of graduations or intensities. In this paper it is always assumed that a rectangular slab represents a (CRG),$(G(X))$. Each node of the slab represents a causal element of a (CRG), $((x^k_{i,j}))$. Each circular plate at a node represents a characteristic or dimension (i). When there are multiple dimensions, they are represented as a collection of circular plates, (i)s at a node. Each circular plate, (i) is divided into $(j \in J)$ slices, representing the intensities of each corresponding dimension. Each line represents a link that is a connection between each $((x^k_{i,j}))$, and $((x^{k'}_{i',j'}))$, for each $((i,j);(i',j');i \neq i', j \neq j')$. The rectangular slab in Figure 3, is an example of (8) causal elements each having (4) dimensions, with each dimension having (4) levels of intensities, $((x^k_{i,j}), k = 1, \cdots, 8; i = 1,2,3,4; j = 1,2,3,4)$. In general, any number of dimensions with any number of intensities for each dimension can be represented. As in the tetrahedron example, only a few lines are outlined. In general all dimensions, and their corresponding intensities are related to each other by straight lines on rectangular slab. The totality of nodes and links constitute networks on each face of the rectangular slab and in the internal region of the slab. The network on each surface of the slab is a network with linear segments or links joining each pair of nodes. The opposing faces causal elements, their dimensions and their corresponding intensities are connected through non-linear segments or curvatures in complex space. If the dual projection of a segment of a (CRG) that contains singularities or (singularity clusters), then there is a search to find a projective dual of the dual segment that is in the complex space between any two opposing faces of the rectangular slab. This dual projective zone in the complex space, contains links of the internal networks that are considered to be non-linear due to multiple forces in action. Dimension and intensity are important elements of the causal networks development on the rectangular slab that represents (CRG).

In general dimension is divided into two categories, integral dimension, and separable dimension. Integral dimension is defined as when one dimension is assigned a value, then it implies that other dimensions must be assigned values that depend on the value of that dimension as well, [7]. If dimensions are not integral, then they are separable, which simply means independent. Separable dimensions acquire values that are not correlated. Though the type of dimension is important in the construction of (CRG), they have no impact on how the dimensions are represented. Their impact is on the occurrence of singularities. Integral dimensions tend to produce non-singularities and separable dimensions tend to produce singularities. When there exists a larger number of causal elements, geometrical representation of larger number of causal elements, is done by attaching several rectangular slabs or tetrahedrons as is shown in Figure 3. New dimensions can be added by adding more circular disks sliced to represent intensities. Dimension determines the degree of causality [8]. The degree of causality corresponds to the position of the dimension of causal elements. There exists a hierarchy of disks based on their level of relevance. Separable dimensions tend to comprise higher level disks, while integral dimensions tend to occupy lower level disks. The position of causal elements, given its' dimension space determines the action. Action is the formation of links in causal networks. Depending on whether the causal networks are dense and compact networks or sparse networks the shape of (CRG) is determined. The shape of (CRG) is determined in the sense that dense causal networks define a (CRG) with strong homeomorphic tendencies. Sparse causal networks are (CRG) with many singularities that renders them unstable. The compactness or sparseness of causal networks affects the position, and the angle of hyperplanes. It is possible to cut out projective segments out of any face of (CRG). Hyperplanes cut subgroups of (CRG) and create projective spaces of each sub-group (CRG). Location of points on the projective

sub-group corresponds to hyperplanes. Location of the points of hyperplane pencils also indicate whether the points are non-singular or singular points depending on the degree of inclination of the pencils. Segments on each face of the rectangular slab are the base of a cone constructed by hyperplane pencils and their dual hyperplane pencils that create the dual projective zone that contains singularity cluster. The dual projective region is the vertex of the cone. Segments with all non-singular points are on cylinders constructed by hyperplane pencils and dual hyperplane pencils that are parallel and are of equal lengths. The same applies to dual projective zones in the complex space. Figure 4, depicts a hierarchical representation of dimension relating to position and geometrical representation of causal elements. Figure 5, is a flow chart summarizing the degree of causality and the orientation of hyperplanes.

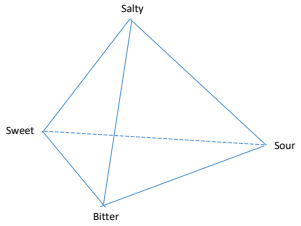

Figure 1. Henning's tetrahedron

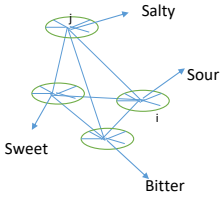

Figure 1a. Henning's tetrahedron representation of one causal element

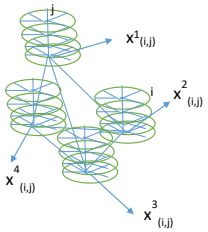

Figure 2. A tetrahedron representing the relationship among causal elements

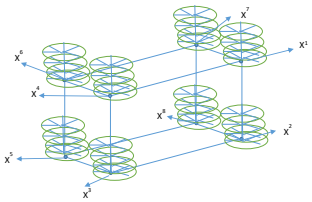

Figure 3. Larger number of causal elements represented as a rectangular slab (case: K=8; I=4, J=4)

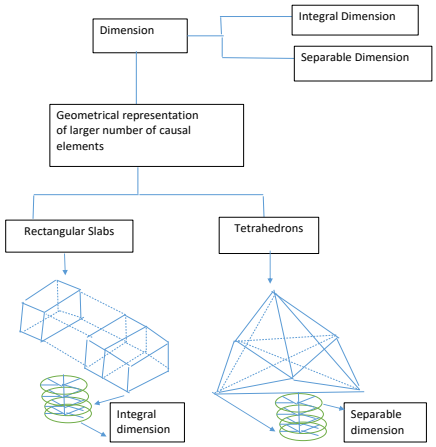

Figure 4. Graphical representation of larger number of causal elements and classifications of dimensions

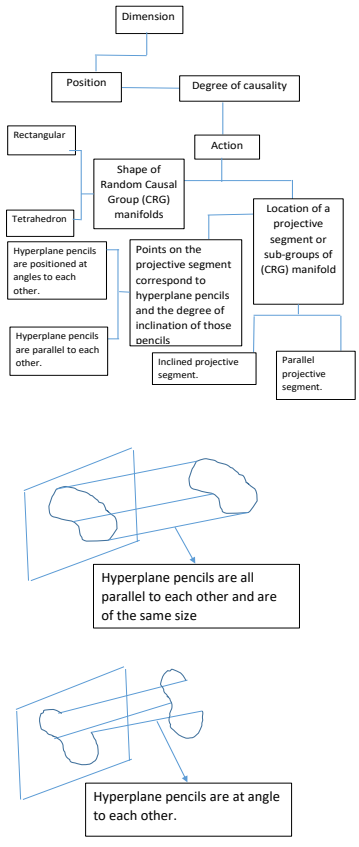

Figure 5. Flow chart depicting causality and hyperplanes

Each geometry, (tetrahedron, rectangular slab) defines a particular topological structure. For example, in the case of a rectangular slab, it represents a presupposition that all (8) causal elements representing the nodes of the rectangular slab, are not considered to be equally positioned with respect to each other. In the case of a tetrahedron if all sides of triangles making up the faces of the tetrahedron, are equal, then it is considered that all causal elements are equally distanced and represent the same level of importance. The choice of the structure of a (CRG) depends on the method of measurement. It is for this reason that those structures are chosen that give a metric space. Since each node is a node of a network, with node coordinates given as the values of each dimensions/intensities denoted by cardinal numbers, then it is easy to calculate distances and measure proximity of each dimension/intensity to the others. The distance, $(d(x^k_{i,j}, x^{k'}_{i',j'}); i \neq i', j \neq j')$ between (2) causal elements is defined as a real valued function. Each face of a (CRG) represented topologically as a rectangular slab is considered to be a network of links connecting dimension/intensities at each node to dimension/intensities of another node as is shown in Figure 6. Each face of a (CRG) is a collection of nodes and links, where each link connects any two nodes $((x^k_{i,j}, x^{k'}_{i',j'}))$. Each node representing a causal element's dimension is presented as a circular disk divided into several slices or wedges that represent intensities. It is assumed that there is a total of (J) intensity levels for each dimension, $(j \in J)$. The number of slices on each circular disk is varied depending on intensity levels. Each circular disk has a center that represents a causal element, $((x^k_{i,j}))$. The node by itself has intensity (zero).

The nodes on the boundary of the circular disk are degrees of intensities measured from (zero). The area of each slice represents the magnitude of the intensity level. A wide slice represents a high intensity level. So the (2) points on the boundary of the circular disk relating to the wide slice are farther apart, which means, that the (2) points are with intensities with very different magnitudes from each other. A narrow slice represents a low intensity level. The (2) points on the boundary of the disk relating to the narrow slice are close to each other, which means that the (2) intensity levels are close to each other or similar, as is shown in Figure 6 and Figure 7. Any two nodes $((x^k_{i,j}, x^{k'}_{i',j'}))$, via their dimensions/intensities are connected by a collection of links, they are then connected by paths as is shown in Figure 8. Thus each face contains a collection of paths. In Figure 8, a sample of a network on face (V^p) is demonstrated. $(G(X))$, is now identified as a (CRG) with geometrical representation, $(G(X, V^p); p = 1, \cdots, P)$, where (p) is the face number, (V) indicates a face, and (P) is the maximum number of possible face numbers. Not all links are included, but the idea of links and paths are clearly established. It is proven that links are homeomorphic. homeomorphism is defined as follows: let (f), and (g) be two continuous maps such that $(f, g : x^k_{i,j} \longrightarrow x^{k'}_{i',j'})$ if $(g = f)$, then the link is homeomorphic. Otherwise, if $(f, g : x^k_{i,j} \longrightarrow x^{k'}_{i',j'})$ and $(g \simeq f)$, then the link is homotopic.

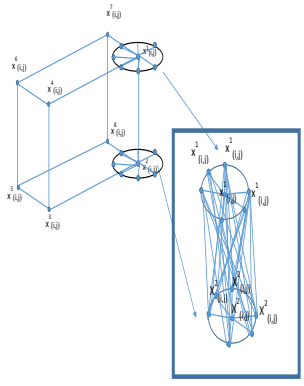

Figure 6. Causal elements with dimension and intensities depicted as networks

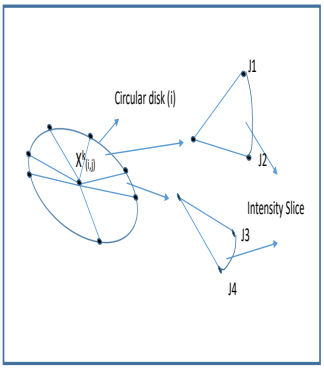

Figure 7. Circular disk representing dimension and its' intensities

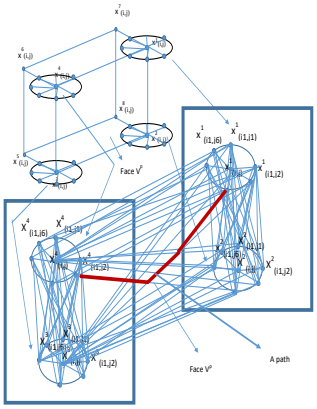

Figure 8. Network of nodes and links constituting paths

Each node is connected to the others through a set of links called a path. Each link is represented by a positive distance denoted as $(d(x^k_{i,j}, x^{k'}_{i',j'}) \geqslant 0)$. These paths are called homeomorphic paths. Homeomorphic paths are paths that share similar patterns, as is shown in Figure 8. In Figure 8, only one path is indicated as a general example. Homeomorphic paths are differentiated into 2 types, those that share at least one link, and those that share no links. Homeomorphic paths that share at least one link contain non-singular points. Homeomorphic paths that share no links may contain singular points. Non-singular points are those points where change in the intensity of one dimension with respect to change in the intensity of another dimension either does not shift the point so it stays on the same path, or it shifts it to another existing path, the concept is denoted as $(\frac{\partial(x^k_{i,j})}{\partial(x^{k'}_{i',j'})} = 0; i \neq i'; j \neq j')$, or $(\frac{\partial(x^k_{i,j})}{\partial(x^{k'}_{i',j'})} = f(x^k_{i,j}, x^{k'}_{i',j'}))$, where $(f(x^k_{i,j}, x^{k'}_{i',j'}); f \in \Re^n)$ is the function representing a linear link in the real space. Singular points are those points where change in the intensity of one dimension with respect to change in the intensity of another dimension shifts the point to a complex region. Figure 8a, demonstrates the path switching action due to the intensity level (j) of each dimension (i). In Figure 8a, the points inside a path are called chain causal points, and are represented as $(y^{(i,i')|(j,j')}_{c_a}, c_a = 1, \cdots, C_a)$, where (C_a) represents the maximum number of chain causal points. The following Theorems demonstrate the homology / homotopy of links and paths.

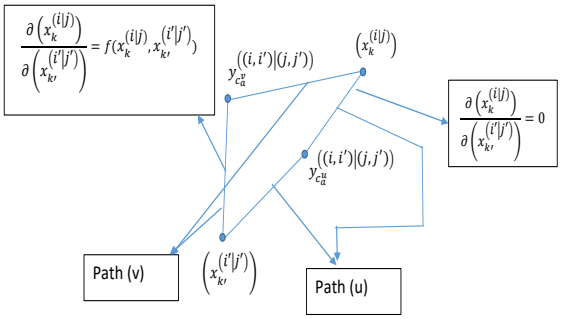

Figure 8a. Shifting paths due to change in the intensity level of a dimension

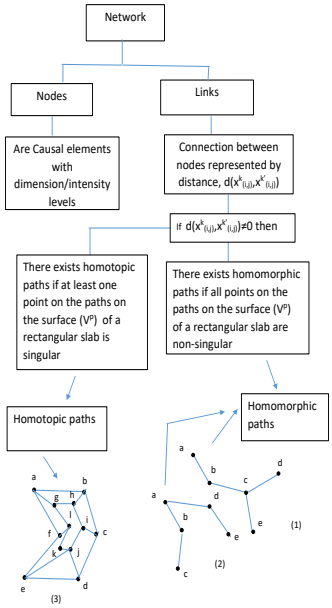

Figure 9. Homomorphic and Homotopic paths

In Figure 9, the formation of links and paths is explained. Again, a network is a collection of nodes, and links connecting every pair of nodes. Nodes are graphical representation of causal elements which are distinguished by their dimensions/intensities. The totality of the networks constituting a rectangular slab represents a (CRG), $(G\{X, V^p\})$. $(V = (V^1, \cdots, V^P))$ represents the faces of the rectangular slab. Each rectangular slab has (6) faces, $(V^1 = V_1^1, \cdots, V_6^1))$. The number of faces increase based on the number of causal elements rectangular slabs as is shown in Figure 4. Each face $(V^p, p = 1, \cdots, P)$ of the rectangular slab, contains a network of links joining entry nodes (x^k) to exit nodes $(x^{k'})$, $(k \neq k')$. Each link is distinguished by its' length (or distance between the corresponding pair of nodes), represented as $(d((x^k_{i,j}), (x^{k'}_{i',j'})) \neq 0)$. All the links that join any origin destination pairs constitute paths. Paths are homomorphic if all points on these paths are non-singular. In Figure 9(1) paths from origin (a) to destinations (d) and (e) are homomorphic. The same functional form is used to go from (a) to (d), and (a) to (e) in Figure 9(1). The same reasoning applies to 9(2). In 9(3), the paths from (a) to (e) are homotopic paths. Paths are homotpoic if there exists at least one singular point. In case 9(3), any point inside region (ghijkl) is a singular point.

Gravitational force $(\delta(i)\mid_j)$ is defined to be the force of attraction of the intensities of each dimension when they interact with each other due to their membership in a (CRG). A gravitational force is equal to the intensity level times the velocity with which it can affect the structure of any (CRG), denoted by $(\delta(i)\mid_j) = (\mid j \mid_i \times \nu_{j|_i}; j \neq j'))$, where $(\mid j \mid_i; j = 1, \cdots, J; \forall(i))$ is the magnitude of intensity of dimension (i) of a causal element, and $(\nu_{j|_i}; j = 1, \cdots, J; \forall(i))$, is the velocity of interaction among (j) intensities of dimension (i). Velocity $(\nu_{j|_i})$ is defined as the change in distance between any two points with respective to a unit change in intensity (j), $(\nu_{j|_i} = \frac{\partial(d((x^k_{i,j}),(x^{k'}_{i',j'})))}{\partial(j)})$ given that (j') stays fixed or in case (j) stays fixed, then the velocity is defined as the change in distance between any two points with respective to a unit change in intensity (j'), $(\nu_{j'|_{i'}} = \frac{\partial(d((x^k_{i,j}),(x^{k'}_{i',j'})))}{\partial(j')})$.

Theorem 2. *Let (f), and (g) be (2) linear functions representing line segments between pairs of points, $(x^k_{i,j}), (x^{k'}_{i',j'})$, as is shown below, on the network on face (V^p), $((f),(g) \in V^p)$, $((f),(g) \in G\{X, V^p\})$. (f), and (g) are homeomorphic functions. All links of the network on face $(V^p \in G\{X, V^p\})$ are homeomorphic line segments.*

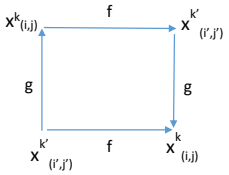

Homeomorphism of (f), and (g)

Proof. Let all entry nodes of a line segment to be in set $(X^* = \{x^k_{i,j}(V^p)\}; X^* \subset X)$ for a specific face (p), and all the exit nodes be in set $(Y^* = \{x^{k'}_{i',j'}(V^p)\}; Y^* \subset X)$, where $(k \neq k')$. Let $(f, g : X^* \to Y^*)$ be any two maps joining a pair of nodes $(x^k_{i,j}(V^p), x^{k'}_{i,j}(V^p))$. (f), is homomorphic to (g), $(f = g)$ if the gravitational forces of the origin and destination nodes are equal $(\delta_j = \delta_{j'}; j \neq j')$ [1]. This means that there exists a function $(F(x^k_{i,j}(V^p), \delta))$ such that $(F(x^k_{i,j}(V^p), \delta) = f(\delta_j))$, and $(F(x^{k'}_{i',j'}(V^p), \delta) = g(\delta_{j'})$. If the gravitational forces of the nodes of a link are not equal,$(\delta_j \neq \delta_{j'}; j \neq j')$, then those links are homotopic, meaning $(f \simeq g)$. In general, if a link can be represented by function $(F(x^k, \delta) : X^* \times \Delta \to Y^*)$, where $(x^k \in X^*)$ is the set of all origin nodes, $(X^* = \{x^k_{i,j}(V^p)\})$, and (Y^*) is the set of destination nodes, $(Y^* = \{x^{k'}_{i',j'}(V^p)\})$, and (Δ) is the space of all possible gravitational forces, $(\delta \in \Delta)$, then $(F(x^k, \delta) = f(x^k, \delta_j))$, and $(F(x^{k'}, \delta) = g(x^{k'}, \delta_{j'}))$, given that $(\delta_j = \delta_{j'})$, thus $(F(x^k, \delta) = F(x^{k'}, \delta))$. This is called the homology condition. In the case of homotopic links where $(\delta_j \neq \delta_{j'})$, it is assumed that for the homology condition to hold, $(\delta_j = \iota \times \delta_{j'})$, the gravitational force at destination node must be a multiple, (ι) of the gravitational force at the origin node. The homology condition is modified to homotopy condition and $(F(x^k, \delta) \simeq f(x^k, \delta_j))$, and $(F(x^k, \delta) \simeq g(x^{k'}, \delta_{j'}))$, since $(f(x^k, \delta_j) \simeq g(x^{k'}, \delta_{j'}))$, thus $(F(x^k, \delta) \simeq F(x^{k'}, \delta))$. □

Paths play an important role in the process of finding stable sub groups of a (CRG). Paths represent,causal chains. Each set of points of a causal chain between any two causal elements is denoted by $(y^{(i,i')|_{j,j'}}_{c_a}; c_a = 1, \cdots, C_a)$. The direction of the links comprised of causal chain points depends on the gravitational force of dimension (i). For example, link $(y^{(i,i')|_{j,j'}}_{c_a}, y^{(i,i')|_{j,j'}}_{c_a+1}); c_a = 1, \cdots, C_a - 1)$ can occur if $(\frac{\delta((i)|_j)(y^{(i,i')|_{j,j'}}_{c_a})}{\delta((i')|_{j'})(y^{(i,i')|_{j,j'}}_{c_a+1})} < 1)$. Causal chains are intermediary nodes representing the process of which any (2) causal elements, $(x^{(i)|j}_k)$, and $(x^{(i')|j'}_{k'})$ can be connected. Note here that an alternative notation is used to denote causal elements. $(y^{(i,i')|_{j,j'}}_{c_a})$s are usually information based, and are complementary causalities

[1] $(\delta_j = (\delta(i)\mid_j))$

leading to the existence of the main causal elements. A segment (W) cut by hyperplanes contains links on several paths. The boundary points of $((W))$ must fall on links of paths, otherwise they can not exist unless they are on causal chains. Hyperplane pencils are used to find homeomorphic segments to segment (W). If hyperplane pencils are at the points of tangent bundles, then every boundary point of segment (W) is a non-singular point, and then every boundary point in the dual projection segment, (W') is a non-singular point. This implies that all the causal chain points connecting causal elements that fall within segment (W), and the causal elements on these paths are stable causal chain points and causal elements, and the segment represents a stable sub-group of a (CRG). If hyperplane pencils and their dual are parallel and are of equal lengths, then the sub-group is both stable and complete. Complete means that there exists no other homeomorphic sub-group that contains extra causal elements outside of the complete and stable set.

Theorem 3. *All paths on face (V^p) are either homeomorphic or homotopic.*

Proof. Let a causal element be alternatively represented as $(x_k^{(i)|j})$, and let causal chain points be represented as $(y_{c_a}^{(i,i')|_{j,j'}})$. Let (u) represent a path such that $(u = \oplus u_r(x_k^{(i)|j}, y_{c_a}^{(i,i')|_{j,j'}}, \delta_j) \oplus u_N(y_{c_a}^{(i,i')|_{j,j'}}, x_{k'}^{(i')|j'}, \delta_{j'}); r = 1, \cdot, N-1)$, where $(u_r(x_k^{(i)|j},\ y_{c_a}^{(i,i')|_{j,j'}})$ is the path from node $(x_k^{(i)|j})$ to node $(y_{c_a}^{(i,i')|_{j,j'}})$, where node $(y_{c_a}^{(i,i')|_{j,j'}})$ represents causal chain nodes between the origin node $(x_k^{(i)|j})$, and the destination node $(x_{k'}^{(i')|j'})$, and (c_a) is the number of causal chain nodes. This representation is equivalent to $(u = \oplus f_r(x_k^{(i)|j}, y_{c_a}^{(i,i')|_{j,j'}}, \delta_j) \oplus f_N(y_{c_a}^{(i,i')|_{j,j'}}, x_{k'}^{(i')|j'}, \delta_{j'}))$, where (f) is defined in Theorem 2. Let (v) represent another path such that $(v = \oplus v_r(x_k^{(i)|j}, y_{c_a}^{(i,i')|_{j,j'}}, \delta_j) \oplus v_N(y_{c_a}^{(i,i')|_{j,j'}}, x_{k'}^{(i')|j'}, \delta_{j'}))$. The equivalent representation is given as $(v = \oplus g_r(x_k^{(i)|j},\ y_{c_a}^{(i,i')|_{j,j'}}, \delta_j) \oplus g_N(y_{c_a}^{(i,i')|_{j,j'}}, x_{k'}^{(i')|j'}, \delta_{j'}))$, where (g) is defined in Theorem 2. Given that the condition exists where $(u_r(x_k^{(i)|j}, y_{c_a}^{(i,i')|_{j,j'}}, \delta_j) = u_{r+1}(x_k^{(i)|j}, y_{c_a}^{(i,i')|_{j,j'}}, \delta_j) = v_r(x_k^{(i)|j},\ y_{c_a}^{(i,i')|_{j,j'}}, \delta_j) = v_{r+1}(x_k^{(i)|j}, y_{c_a}^{(i,i')|_{j,j'}}, \delta_j))$, then by Theorem 2, if the two functions (f), and (g) are homemorphic, $(f = g)$, then there exists a homeomorphism $(F(u, \delta) : v \times \Delta \to u)$, such that $(F(u, \delta) = f(u, \delta))$, and $(F(v, \delta) = g(v, \delta))$, where $(\delta \in \Delta)$, (Δ) is the space of all possible gravitational forces. In the case of homotopic paths, when by Theorem 2, the two functions (f), and (g) are homotopic, $(f \simeq g)$, then $(F(v, \delta) \simeq f(u, \delta))$, and $(F(v, \delta) \simeq g(u, \delta))$. □

The existence of homotopic paths is the reason why singularity occurs. Singularity occurs when change in the position of a causal element $(x_k^{(i)|j})$ on a homomorphic path (u), with respect to change in the gravitational force (δ), $(\frac{\partial u(x_k^{(i)|j}, x_{k'}^{(i')|j'}, \delta(i,i'))}{\partial(\delta(i'))})$, would either shift the causal element $(x_k^{(i)|j})$ to another homomorphic path, to (v), or would shift it to a position outside of any homeomorphic path. In this case, one must assume that the initial path (u), was homotopic. When all causal elements are on homeomorphic paths, then they are considered to be non-singular points. Therefore, all points on a path are non-singular if $(\frac{\partial u(x_k^{(i)|j}, x_{k'}^{(i')|j'}, \delta(i,i'))}{\partial(\delta(i'))} = y_{c_a}^{(i,i')|_{j,j'}})$, path (u) is homomorphic to path (v),$(u \times \Delta \to v)$. If path (u) is homotopic to path (v), then $(\frac{\partial v(x_k^{(i)|j}, x_{k'}^{(i')|j'}, \delta)}{\partial(\delta)} = z_{s_d}^{(q-s)}; (n-k) \leq s_d \leq n)$, (n) is the total number of possible causal elements in $(\Re^n)$, and (k) is the number of non-singular causal elements before the occurrence of singularity. (q) is the dimension of the parallax causal element that is related to the dimension or characteristics of causal elements (i). (q) is a function of dimension (i), $(q = \beth(i))$. $(s > 0)$ is a positive number representing those dimensions that belong to non-singular causal elements before the singularity. The causal element $(z_{s_d}^{(q-s)})$ is called the parallax causal element. The set of parallax causal elements is denoted by $(z = \{z_{s_d}^{(q-s)}\})$.

Parallax causal elements, [10] are the transcendental transformation or transcendental illusion or transcendental dialectic of singularity. Transcendental refers to what is assumed about the causality of the original casual elements in singular zones which is required in order find a valid zone in the internal networks. Illusion in this context refers to how understanding, and rationality impacts the perception of causal elements as it relates to singular zones. Therefore, Parallax causal elements are the original causal elements that are looked at from a new angle of understanding and rationality, that sorts out the dimension property

of original causal elements, so that only some dimensions are deemed important or relevant. This explains the choice of dimension, $(q-s)$. The internal networks space is considered to be a Parallax gap. Parallax gap is a space shared by both the Parallax causal elements, and the original causal elements, in as much as the parallax gap is a space that shows the other side of the original causal elements space. Thus, the naturally, parallax gap is in the complex space, which mirrors the original causal elements space which is in the real space. In short, transcendental dialectic is what singularity would look like if it were perceived through a different set of dimensions than what is expected. Parallax causal element can be found by shifting the perspective of a singularity. This perspective is a parallax gap, and lies in the complex space, $(\mathbf{Z}^n)$, or in this case the internal network. The parallax causal element $(z_{s_d}^{(q-s)})$ is neither on path (u) nor on it's homotopic path (v), but change in the position of the causal element $(x_k^{(i)|j})$ with respect to change in the gravitational force (δ) would shift the perspective of a singularity to a complex space, $(z_{s_d}^{(q-s)} \in \mathbf{Z}^n)$.

The Parallax causal element thus found is in the internal network, in other words, it is inside the rectangular slab representing (CRG), as is shown in Figure 10. The singularity becomes a set of parallax causal elements in the internal network. A parallax causal element is formulated as (1): $(z_{s_d}^{(q-s)} = \delta(q-s) \times x_{n-k}^{(q-s)} + ii \times \eta(\delta(q-s), \delta(q'-s)\xi_{m_d}^{(q-s)}; m_d = 1, \cdots, M_d; i-1 \leq q \leq I; i = 1, \cdots, I-1; ii = -1; s_d = n-k, \cdots, n)$, where $(x_{n-k}^{(q-s)} \in \Re^n)$ is the real part equal to the causal element not in the set of non-singularities of segment $(W \in \Gamma^{(i)})$, and $(\xi_{m_d}^{(q-s)} \in \mathbf{Z}^n)$ is the induced causality, and (m_d) is the number of induced causal elements that constitute a causal chain between Parallax causal elements and the (origins ,destination) pairs of non-singular causal elements on the faces of the rectangular slab. (n) is the universe of all possible causal elements. Induced causality is causality that exists due to the influence of factors linking to the (CRG), from outside, normally not easily detectable. An example of induced causality is the impact of gravitational force covariances on the length of the curvature of the links of the internal networks. It is assumed that due to induced causality factor all the links in the internal networks are arcs. $(\eta(\delta(q-s), \delta(q'-s); (i-1) \leq q \leq I; i = 1, \cdots, I; s \leq 0)$ is the covariance between the gravitational forces of the dimensions of origin Parallax causal element $(q-s)$, and the gravitational forces of the dimensions of destination Parallax causal element $((q'-s); q \neq q')$. The initial Parallax causal element $(z_{n-k}^{(q-s)})$ is formulated as $(z_{n-k}^{(q-s)} = \delta(q-s) \times x_{n-k}^{(q-s)} + ii \times \eta(\delta(q-s), \delta(q'-s)\xi_1^{(q-s)}; m_d = 1, \cdots, M_d)$, where the first induced causal element $(\xi_1^{(q-s)} = C)$, and (C) is an arbitrary positive number that represents the magnitude of the parallax gap. Induced causal elements $(\xi_{m_d}^{(q-s)})$ are formulated as, $(\xi_{m_d}^{(q-s)} = \delta(q-s) \times z_{n-k}^{(q-s)} + ii \times \eta(\delta(q-s), \delta(q'-s) z_{s_d+1}^{(q'-s)}; s_d = (n-k), \cdots, n)$. The dimension of the induced causal element, $(\xi_{m_d}^{(q-s)})$ depends on the location of the induced causal element point on the arc, $(z_{s_d}^{(q-s)}, z_{s_d+1}^{(q'-s)})$. Close to the origin node and up to the middle of the arc, the dimension of $(\xi_{m_d}^{(q-s)})$, is the same as the origin node, $(z_{s_d}^{(q-s)})$. Past the middle point, the dimension of $(\xi_{m_d}^{(q-s)})$, must be equal to the dimension of the end node, $(z_{s_d+1}^{(q'-s)})$.

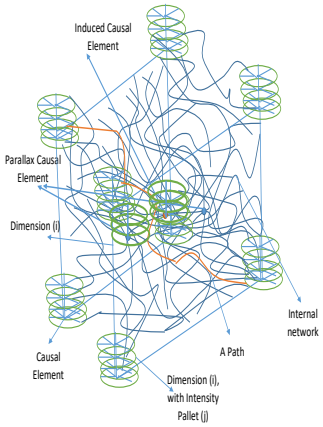

Figure 10. Internal networks

The internal networks inside of the rectangular slab represents networks with (start, and exit) nodes, $((x_k^{(i)|j}, x_{k'}^{(i')|j'}) \in \Re^n)$ from opposing faces $(V^p, V^{p'})$, where $(V^{p'})$ is the opposing face of (V^p). Internal networks are in the complex domain since the curvature of the links can not be determined solely in the real domain, $(\Re^n)$. The impact of gravitational force covariances on the curvature is expressed quantitatively in the complex field, $(\mathbf{Z}^n)$. It is not realistic to assume that the links of the internal networks should be line segments. It is reasonable to assume that all links are arcs due to gravitational effects. The degree of non-linearity depends on the level of the attractiveness of each pair of origin and destination nodes and the gravitational force covariances. Due to gravitational force covariances, non-linear segments in internal networks are either homeomorphic or homotopic. The difference between links in $(\Re^n)$ and arcs in $(\mathbf{Z}^n)$ is that homemorphisom or homotopy in $(\Re^n)$ space depends on one factor, the intensity level (j), and impacted by the gravitational forces, while homeomorphism or homotopy in $(\mathbf{Z}^n)$ depends on two factors, gravitational forces, and the gravitational force covariances. Internal networks contain non-linear paths. It is also shown that these non-linear paths are either homeomorphic or homotopic. Non-linear paths joining causal element points, $((x_k^{(i)|j}, x_{k'}^{(i')|j'}) \in \Re^n)$, in opposing faces of the rectangular slab, contain intermediate Parallax causal points $(z_{s_d}^{(q-s)})$ in complex space, $(\mathbf{Z}^n)$. Internal network paths are represented by $(\pi_z \in \mathbf{Z}^n)$. The curvature and the shape of the curve (convex, concave) between any two points in the interior of complex space depends on the magnitude of the gravitational force of the (start, exit) causal elements, $(\delta(i), \delta(i'))$, and the gravitational force of the interior nodes, $(\delta(q-s), \delta(q'-s))$, and the gravitational force covariances among interior nodes, $(\eta(\delta(q-s), \delta(q'-s)))$. The following two theorems prove the conditions for the existence of homotopy of non-linear arcs and paths of the interior networks. The particularity of the internal network is that though the points inside lie in the complex domain, the points on the opposite faces, $((V^p, V^{p'}), p \neq p')$ are in the real domain, $((x_k^{(i)|j}, x_{k'}^{(i')|j'}) \in \Re^n)$. This means that the origin node and the destination node of a path in the internal network are in the real domain, and thus can be easily identified. The Parallax causal elements can potentially be identified using formula (1), with potential candidates, $(x_{n-k}^{(q-s)})$. This is not the case for the induced causal nodes in the internal network, $(\xi_{m_d}^{(q-s)})$,where $(m_d = 1, \cdots, M_d)$ is the number of induced causal intermediate nodes between any two Parallax causal elements $((z_{s_d}^{(q-s)}, z_{s_d}^{(q'-s)} + 1); s_d = n-k, \cdots, n)$, and where $(\xi_{m_d}^{(q-s)} = \delta(q-s) \times z_{n-k}^{(q-s)} + ii \times \eta(\delta(q-s), \delta(q'-s)) \times z^{(q'-s)_{s_d}+1})$, where $(\delta(q-s))$ is the gravitational force of the start parallax causal element node of a link, and $(\eta(\delta(q-s), \delta(q'-s)))$ is the covariance between the start, and the end $(z_{s_d+1}^{(q'-s)})$ Parallax nodes. Figure 10a, demonstrates the positioning of the induced causal elements.

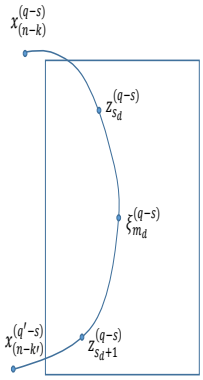

Figure 10a. The positioning of the induced causal elements

Theorem 4. *All arcs in the internal network in complex space, ($\boldsymbol{Z}^n$) are either homeomorphic or homotopic curve segments.*

Proof. If all arcs are generated by a gravitational force, $(\delta(q-s))$, where dimension $((q-s))$ is chosen at random or in other words are independent dimensions with dialectic dependency, and the covariance of gravitational forces $(\eta(\delta(q-s),\delta(q'-s))$ exists for any random dimension, $((q-s))$, then each arc is generated by a function (F_z) such that $(F_z(0,z_{s_d}^{(q-s)}) = z_{s_d}^{(q-s)}))$; and $(F_z(z_{s_d+1}^{(q'-s)},1) = z_{s_d+1}^{(q'-s)})$ for any function $(F_z : \mathbf{Z}^n \times \mathbf{I} \to F_z)$ in (I) space is homeomorphic to space, $(\mathbf{Z}^n)$. The arcs generated this way are homotopic to each other. If arcs are generated by a family of gravitational forces $(\delta(q-s))$, and covariance of gravitational forces $(\eta(\delta(q-s),\delta(q'-s))$, where all dimensions $((q-s))$ belong to a dependent families of dimensions, where gravitational forces, and covariance of gravitational forces stay within fixed limits, then all arcs generated by any function (F_z) are homeomorphic to each other. □

Theorem 5. *All paths in the internal network in complex space, ($\boldsymbol{Z}^n$) are either homeomorphic or homotopic mappings.*

Proof. Let $(\pi_z \in \mathbf{Z}^n)$ denote a path mapping node $(z_{s_d}^{(q-s)})$ to node $(z_{s_d+m}^{(q'-s)}; m \geq 0)$. Theorem 4, can be extended to mappings. A mapping, (π_z) is a chain homotopy $(F_z(z_{s_d}^{(q-s)}) \to F_z(z_{s_d+m}^{(q'-s)}))$ if $(\delta(q-s))$, and $(\eta(\delta(q-s),\delta(q'-s))$, include random dimensions $((q-s))$, with dialectic dependency for a chain of links on the mapping of an origin node $(z_{s_d}^{(q-s)})$ to any destination node $(z_{s_d+m}^{(q'-s)})$. A mapping (π_z) is a chain homology if $(\delta(q-s))$, and $(\eta(\delta(q-s),\delta(q'-s))$, belong to dependent families of dimensions, where gravitational forces, and covariance of gravitational forces stay within fixed limits, for a chain of links on the mapping of an origin node $(z_{s_d}^{(q-s)})$ to any destination node $(z_{s_d+m}^{(q'-s)})$, then all paths generated by any mappings (π_z) are homeomorphic to each other. □

A (CRG), $(G(X,V^p); p = 1,\cdots,P)$ is represented by a rectangular slab each with (8) faces (V^p). Each node of the rectangular slab represents a causal element, $(x_{i,j}^k(\delta,\eta), k = 1,2,,\cdots,K; i = 1,\cdots,I; j = 1,\cdots,J)$, where each node consists of circular disks that represent dimension (i) of each (k) causal element. Circular disks are divided into (j) slices. Each (j) is a level of intensity of each (i). Based on the gravitational force of each (i), which depends on (j), each causal element reacts with another causal element by creating links that connect each $(j \neq j')$ of $(i \neq i')$ to each (j') of (i'). This way, there exists networks of nodes, and linear links connecting these nodes on each face of the rectangular slab. Hyperplanes in a hyperplane space (L^i), and hyperplane pencils, (Γ^i) are tools used to cut sections (regions) on faces (V^p). These regions are denoted by $(W \in \Re^n)$, with boundary points $(\beta(W))$ which are the points cut by hyperplanes on face (V^p).

Each region (W) is of dimension (i) since hyperplanes are the projective spaces containing sections (W). Let the dual space of the projective space hyperplanes,(L^i) be denoted as (L'^i), and the dual hyperplane pencils be denoted as (Γ'^i), and let the dual of region (W) be denoted as $(W' \in \Re^n)$. The object of the dual space is to represent the region (W) on a linear space as homeomorphic to the projective space. If all the boundary points $(\beta(W))$ are non-singular then the projective space points in the real space and all points on the boundary of the projective dual segment, $(\beta(W'))$ are homeomorphic to the points of $(\beta(W))$.

Hyperplanes become tangent hyperplnes with dimension not greater than (i-1), if all the hyperplane pencils are tangents to $(\beta(W))$. In the case when tangent hyperplanes can not be found, then the dual segment falls in the complex space, $(\mathbf{Z}^n)$. It is assumed that there exists at least one singular point among the boundary points $(\beta(W))$. Therefore, the dual boundary points, $(\beta(W'))$ fall in the complex space. In the graphical representation, the hyperplanes are shown as a collection of hyperplane pencils cutting regions (W) on face (V^p) as is shown in Figure 11(a), with the dual region (W') depicted as situated on the elevated portion of hyperplanes. In Figure 11(b), the dual region (W'_z) is situated in the internal networks inside of the rectangular slab, in complex space. The dual region (W'_z) cuts a section in the internal networks. The boundary points $(\beta(W'_z))$ are points on arcs on paths of the internal networks. If these points are the points of tangent hyperplanes, or tangent geodesic hyperplanes, then all the points on the boundary $(\beta(W'_z))$ are non-singular points; otherwise if the points are not the points of tangent geodesic hyperplanes, then there exists at least one singularity. In this case, search for non-singularity continues by cutting other sections in the internal networks and applying geodesic hyperplanes, and checking for singularities. This search should continue until non-singular sections are found that lead to stable causal elements. All non-singular points indicate that the links where the boundary points $(\beta(W'_z))$ are on, are links of paths or mappings that connect causal elements on the faces (V^p), and these causal elements are highly stable and relevant to a (CRG). The causal elements thus found are stable, and complete. Therefore, any (CRG) made up of thus found causal elements is invariant in nature, and is complete. In this case, the hyperplane pencils are parallel to each other and are of the same size. In general, the boundary points $(\beta(W'_z))$ must fall on the links of the paths in the internal network, if those points are non-singular. Singularities occur when the boundary points fall outside of the paths.

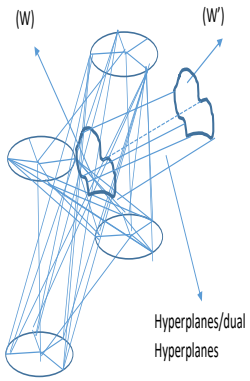

Figure 11a. Hyperplanes cutting region (W), and its' dual region (W')

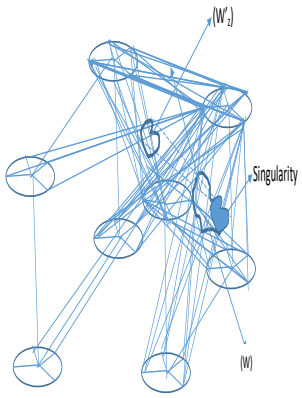

Figure 11b. Dual region (W') with a singularity zone, and its' dual region (W'_z) inside the rectangular slab

The use of the hyperplanes tool is to examine the stability of the networks on face (V^p). Stability refers to finding out the relevancy of the causal elements in making up a (CRG). Any section (W) is stable if hyperplanes cut points on the boundary $(\beta(W))$, all of which are non-singular points, otherwise, if there exists at least one singular point on $(\beta(W))$, then (W) is not stable. In the case of instability, hyperplanes point to a dual of (W), $(W'_z \in \mathbf{Z}^n)$ in complex space, $(\mathbf{Z}^n)$.

3 Hyperplanes and Singularities, and search for stability

The objective is to find a subgroup of a (CRG) that is stable. Stable implies that all the causal elements that constitute these subgroups are irreducible, in which case there exists a strong gravitational attraction among the causal elements with a set of characteristics (i), also covariance among the causal elements exists and is significant. In order to find a subgroup of a (CRG) that is at equilibrium or stable, one must use a particular tool. Tools used here are hyperplanes and hyperplane pencils. Next, one must use a technique as follows: singularity detection by using hyperplanes to cut segments to be tested for singularity testing, transition phase (the internal network in complex space, if singularity occurs), repeat search for singularities in the transition phase if non-singularity not found, and continue until a region is found that is irreducible, (all non-singular points). This is what happens during the transition phase, in the complex space, $(\mathbf{Z}^n)$; two cases can occur. In case one, given section (W), on face (V^p), with at least one singularity, the dual of (W), (W'_z) in the interior network contains all network arcs with boundary points, $(\beta(W'_z))$, that are all non-singular, then the links in the dual section (W'_z), are on paths that map the origin causal elements to the destination causal elements, $((x^k_{i,j}) \in \Re^n \rightarrow x^{k'}_{i',j'}))$ in the real space, $(\Re^n)$. In case one, the causal elements at the origin and destination of these paths are irreducible elements of a sub group of a (CRG).

In case two, given section (W), on face (V^p), with at least one singularity, the dual (W'), has a dual (W'_z) in the internal networks contains all network arcs with boundary points, $(\beta(W'_z))$, at this point two possibilities can occur. Either all boundary points are non-singular or there exists at least one point which is singular. The dual of (W'_z), (W''_z), is found by applying hyperplanes tools, and checking for singularity. As long as singularity exists, case two is repeated and search for non-singularity continues. Hyperplanes and hyperplane pencils exist in the real space $(\Re^n)$, and are transformed into curved manifolds consisting of geodesics curves in the complex space $(\mathbf{Z}^n)$. Geodesics,$(\Lambda^{(q-s)})$ are the complex space version of hyperplane pencils. (CRG) is depicted as a rectangular slab for reasons of simplicity of visualization, and clarity of conceptualization, it is assumed that all faces of the rectangular slab are in the real domain, and the space

between the opposing faces lies in the complex domain. Therefore it is possible to cut sub regions on the faces using real domain hyperplanes, and hyperplane pencils, and in the internal regions with geodesics. Since hyperplanes are considered to exist in a projective space as dual hyperplane pencils that projects the dual region onto the projective space in $(\Re^n)$, then, in case of singularity, the dual region also possess its' own dual in the projective space in $(\mathbf{Z}^n)$. The duality region and the dual hyperplanes are shown in Figure 11a, and the dual of the dual region and its' corresponding geodesics are shown in Figure 12b. Most simple sub region selection would be a circular form, but to cover all possible subregions on a face of a rectangular slab, irregular shape regions could be cut using hyperplanes, as is shown in Figure 12a.

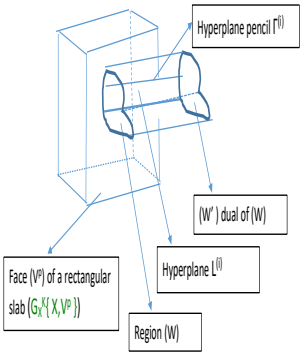

Figure 12a. Region cut by hyperplanes with all non-singular points

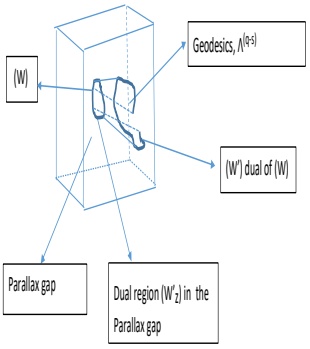

Figure 12b. Dual region in the complex space cut by geodesics

In Figure 12a, (CRG), $(G(X, V^p))$, is depicted as a rectangular slab, on one face (V^p), region (W) is cut using hyperplane pencils (Γ^i). Hyperplanes are formulated as a collection of hyperplane pencils, $(L^i = \oplus\Gamma^i)$. The projection of these hyperplanes are dual hyperplane pencils, $(L'^{(i)})$ create dual region (W'). Figure 11b, depicts the same region (W) cut by hyperplane pencils, except that there exists singularity which is shown on the dual region as an empty space. The hyperplane pencils (Γ^i) are homeomorphic to their dual $(\Gamma'^{(i)})$, and

the hyperplanes (L^i) are homeomorphic to their dual, $(L'^{(i)})$. Region (W) is homeomorphic to its′ projective dual region (W'), if both regions contain the same number of points, in other words, if the intersection $(W \cap \Gamma^i)$ contains the same number of points as the projective dual, $(W' \cap \Gamma'^{(i)})$; otherwise, if the projective dual region has less points, then there exists singularity. If all points of the intersection $(W \cap \Gamma^i)$ are non-singular, then, there exists tangents or fibre bundles, (T^{q-s}), where $(T^{q-s}; (i-1) \leq q \leq I; i = 1, \cdots, I-1)$ such that $(\Gamma^i \times T^{q-s} = 0)$. If the derivative of hyperplane pencils with respect to gravitational force $(\delta(i) \mid_j)$ exists, then the tangent fibre bundles are formulated as,$(T^{q-s} = \oplus(\frac{\partial(\Gamma^i(\delta(i)))}{\partial(\delta(i)}))$. The same applies to the dual segment (W'), where non-singular points exist, $(\Gamma'^i \times T^{q-s-r} = 0; r \geq 0)$. The points on the boundary of the dual segment $(\beta(W'))$ are in the multiplicative space $(\Gamma'^{(i)} \times T^{q-s-r} = 0)$. If on the other hand, the derivative does not exist, then the hyperplane pencils have cut singular points on the region $(W \cap \Gamma^i)$. In that case the dual of hyperplane pencils, $(\Gamma'^{(q-s)})$, and dual hyperplanes $(L'^{(q-s)})$ form a cone with $(W' \cap \Gamma'^{q-s})$ as the base, and the dual region $(W'_z \cap \Lambda^{(q-s)})$, where $(\Lambda^{(q-s)})$, is an arbitrary geodesic pick in the singularity zone of the dual segment, (W'). Repeated arbitrary geodesics, $(\Lambda^{(q-s)})$, form a collection that hit networks in the internal networks, and carves out a zone, (W'_z) containing the points of the intersection of the geodesics and the links of the internal networks. Zone, (W'_z), is the vertex of the projective dual region (W') which is the base of the cone formed by geodesics.

Hyperplane pencils can be formulated as $(\Gamma^i = \alpha_k^{(i)|_j} \times x_k^{(i)|_j}(\delta(i) \mid_j, \tau(j) \mid_i) + \alpha_{k'}^{\prime(i')|_{j'}} \times x_{k'}^{\prime(i')|_{j'}}(\delta(i') \mid_{j'}, \tau(j') \mid_{i'}))$, where (i') is the dual of (i), and $(\alpha_k^{(i)|_j})$, and $(\alpha_{k'}^{\prime(i')|_{j'}})$ are the coefficients of causal elements $(x_k^{(i)|_j}(\delta(i) \mid_j, \tau(j) \mid_i))$, and its′ projective dual point $(x_{k'}^{\prime(i')|_{j'}}(\delta(i') \mid_{j'}, \tau(j') \mid_{i'}))$. The variable $(\tau(j) \mid_i)$ is similar to the variable $(\delta(i) \mid_j)$; as the variable $(\delta(i) \mid_j)$ represents the gravitational force of dimension (i), the variable $(\tau(j) \mid_i)$ is considered to be the causality force of the intensity level (j) of causal element $(x_k^{(i)|_j}(\delta(i) \mid_j, \tau(j) \mid_i))$. The causality force is the covariance between different intensity levels (j) of dimension (i). A hyperplane is formulated as $(\oplus a_k^{(i)|_j} \times \Gamma^{(i)} = L^{(i)} = 0)$. $(a_k^{(i)|_j} = \{\alpha_k^{(i)|_j}\})$ is the coefficient of the hyperplane pencil. The hyperplane exists as long as the Jacobian criterion, (JJ) holds. (JJ) is the derivative of hyperplane pencils with respect to both the dimensional gravitational force, $(\delta(i) \mid_j)$, and the intensity level causality force $(\tau(j) \mid_i)$, and is formulated as $(JJ := (\frac{\partial(\Gamma^{(i)}(\delta(i)|_j, \tau(j)|_i))}{\partial(\delta(i)|_j, \tau(j)|_i)})$.

Hyperplanes cut regions with non-singular points when the Jacobian criterion holds. Singularity occurs when the Jacobian criterion is not satisfied. In that case, for some regions, $(JJ := (\frac{\partial(\Gamma^{(i)}(\delta(i)|_j, \tau(j)|_i))}{\partial(\delta(i)|_j, \tau(j)|_i)})$, the derivative does not exist in the real domain $(\Re^n)$, but the derivative exists in the complex domain,$(\mathbf{Z}^n)$; in other words, the Jacobian criterion is equal the derivative of geodesics with respect to the gravitational forces, and the covariances of the gravitational forces, formulated as, $(JJ := (\frac{\partial(\Lambda^{(q-s)}(\delta(q-s), \eta(\delta(q-s), \delta'(q'-s)))}{\partial(\delta(q-s), \eta(\delta(q-s), \delta'(q'-s))})$. Gravitational forces, and the covariances of the gravitational forces, define the formulation of a Parallax causal element node as, $(z_{s_d}^{(q-s)} = \delta \times x_{n-k}^{(q-s)} + ii \times \eta(\delta, \delta')\xi_{m_d}^{(q-s)}; m_d = 1, \cdots, M_d; (i-1) \leq q \leq I; i = 1, \cdots, I-1; ii = -1)$ in the internal networks. The length of each hyperplane pencil in $(\Re^n)$, is denoted as $(\mid \Gamma^i \mid)$. The length of each hyperplane pencil is the same for all regions (W), and their projective dual region (W'), when all points on the the intersection, $(W \cap \Gamma^i)$ and $(W' \cap \Gamma'^i)$ are non-singular points. Hyperplane pencils have all the same length, $(\mid \Gamma^i \mid = \mid \Gamma'^i \mid)$ if they are orthogonal, $(\Gamma'^i \times T^{i-1} = 0)$ to fiber bundles, (T^{i-1}). Any region that contains boundary points, $(\beta(W'))$ that are in the multiplicative space, $(\Gamma'^i \times T^{i-1} = 0)$ are all son-singular points, and causal elements relating to these points are irreducible. The fibre bundles, (T^{i-1}) have the same length $(\mid T^{i-1} \mid = \mid \delta(i) \mid_j \mid)$, when $(\delta(i) \mid_j = \delta(i) \mid_{j'})$, and all the intensity level causality forces $(\tau(j) \mid_i = \tau(j') \mid_i = BB)$, are fixed at an arbitrary value (BB). On each face of the rectangular slab $(G(X, V^p))$, where all causal elements $(x_k^{(i)|_j}(\delta(i) \mid_j, \tau(j) \mid_i))$, are in the real domain, $(\Re^n)$, when singularities occur, then the dual hyperplane pencil $(\Gamma_*'^{(q-s)})$ that does not obey the Jacobian criterion is a tensor that points to the interior of $(G(X, V^p))$. Here the (*) sign is used to distinguish this particular hyperplane pencils from the others. Due to the effect of gravitational forces acting inside the rectangular slab, the arbitrary hyperplane pencil, $(\Gamma_*'^{(q-s)})$ becomes a geodesic (Λ^{q-s}). Dimension $(q-s)$ represents the dimension of the

singularity, and (s) is considered to be the number of dimensions that correspond to non-singular points of the dual region (W'). It points to a section inside and is a guide to find all geodesics with similar curvatures to cut out an initial zone of interest in the complex domain of the interior networks of $(G(X, V^p))$. Therefore, initially, the choice of the cut is arbitrary, since the geodesic tensor, (Λ^{q-s}) does not indicate a specific point, and therefore some arbitrary region around it is considered.

Lemma 1. *Any hyperplane (L^i) cuts non-singular points in $(W \cap \Gamma^i)$ if the Jacobian criterion, $(JJ \neq 0)$ for hyperplane pencils (Γ^i) is satisfied, and the points on the intersection $(W \cap \Gamma^i)$ are on the network on any face of the rectangular slab.*

The embedded implication is that the existence of Lemma 1, is equivalent to stating that if the gravitational force of dimension (i), $(\delta(i) \mid_j >> 0)$ is very strong, then hyperplanes, $(L^{(i)})$ cut sections, $(W \cap \Gamma^i(\delta(i) \mid_j))$, with all non-singular points. Plus if the gravitational force $(\delta(i) \mid_j >> 0)$ is strong, then it is strong for any finite dimension $(i < \infty)$, and any finite intensity level $(j < \infty)$, in particular for cases when dimension $(i \leq I)$ is finite with an upper limit, and when the intensity level $(j \leq J)$ is finite with an upper limit. (I), and (J), are maximum values of dimension and intensity levels. Strong gravitational force of dimension (i), $(\delta(i) \mid_j >> 0)$, cuts non-singular points $(W \cap \Gamma^i(\delta(i) \mid_j))$, which are irreducible, implying that the maximum values of dimension of the dual region, $(W' \cap \Gamma'^i))$, is $(dim(W') = I' = I)$, the same as section (W).

Lemma 2. *Any number $(K < \infty)$ of causal elements with any number of characteristics or dimensions $(I < \infty)$ and any number of intensity levels $(J < \infty)$ create dense networks. Hyperplanes with large dimensions (L^i) cut a finite number (n_d) of non-singular points on the intersection $(W \cap \Gamma^i)$.*

Lemma 3. *Any number $(K < \infty)$ of causal elements with any number of characteristics $(I < \infty)$ and any number of intensity levels $(J < \infty)$ create dense networks. Hyperplanes, (L^i) with large dimensions cut a finite number of singular points, (s_d), where $(s_d < n_d)$ on the intersection $(W \cap \Gamma^i)$.*

Lemma 3 is equivalent to stating that if the gravitational force of dimension (i), $(\delta(i) \mid_j > 0)$ is medium strength, then the hyperplanes, (L^i) cut at least one singular point, $(W \cap \Gamma^i; i \leq I; j \leq J)$. Here, the dimension of the dual $(W' \cap \Gamma'^{q-s}))$, is $(dim(W') = I' < I)$, is less than section (W).

Lemma 4. *For any number $(K < \infty)$ of causal elements with any number of characteristics $(I < \infty)$ and any number of intensity levels $(J < \infty)$, the dual hyperplanes with large dimensions (L'^i) cuts a finite number of non-singular points, (n_d), on the intersection of the dual region (W') with dual hyperplane pencils (Γ'^i), $(W' \cap \Gamma'^i)$.*

Lemma 5. *For any number $(K < \infty)$ of causal elements with any number of characteristics $(I < \infty)$ and any number of intensity levels $(J < \infty)$, the dual hyperplanes with large dimensions (L'^i) cuts a finite number of singular points, $(s_d < n_d)$, such that the dual projective intersection of the dual region (W'_z) with dual hyperplane pencils $(\Gamma'^{(q-s)})$, $(W'_z \cap \Gamma'^{q-s})$ is the vertex of a cone with base $(W' \cap \Gamma'^{q-s})$, the singularity zone of the dual zone (W'), and where dimension, $(q - s)$ is the dimension of the singularity zone, $((i-1) \leq q \leq I; i = 1, \cdots, (I-1))$, minus the dimension of non-singularity points of the dual region, (W').*

Proof. There are 2 cases: case 1, is when the hyperplanes (L^i) consists of all hyperplane pencils (Γ^i), where the Jacobian criterion $(JJ \neq 0)$, the intensity level causality force $(\tau(j) \mid_i \neq 0)$, and the gravitational force of dimension (i), $(\delta(i) \mid_j \neq 0)$ are both positive. Let the points $(\overline{x} = (x_1, \cdots, x_{n_d}))$ be in the cut segment$((W \cap \Gamma^i(\delta(i) \mid_j))$. By Lemma 4, these points, $(\overline{x})$ are all non-singular points. The dual segment,$(W' \cap \Gamma'^{(i)})$ consists of all non-singular points. Case 2, is when there exists singular points. In this case the hyperplanes (L^i) is not orthogonal to tangent bundles $(T^{(i-1)})$, and tangent bundles do not exist for a collection of points that constitute the boundary points, $(\overline{h} = (h_1, \cdots, h_{s_d}))$ of a singular zone, where $(\overline{h} \in (W' \cap \Gamma'^{q-s}))$. In this case, the hyperplane pencil, $(\Gamma'^{(q-s)})$, has dimension $((q-s); (i-1) \leq q \leq I; i = 1, \cdots, (I-1))$, which is the dimension of the singular zone. In the case of singularity, $(\tau(j) \mid_i = 0)$, $(\delta(i) \mid_j = 0)$ are equal to zero. The dual projection, (W'_z) of the dual region, (W') is in the internal networks. $((W'_z \cap \Lambda^{q-s}))$ is a vertex of

a cone found by geodesics (Λ^{q-s}) with the same number of dimensions $((q-s))$, as the hyperplane pencil $(\Gamma'^{(q-s)})$. The base of the cone is the singular zone of the dual region $(W' \cap \Gamma'^{q-s})$.

□

The dual region in the internal networks, $((W'_z \cap \Lambda^{(q-s)}) \in \mathbf{Z}^n)$, where geodesics $(\Lambda^{(q-s)})$ cut points $(\overline{z} = (z_1, \cdots, z_{s_d}))$ in the networks within the region (W'_z). $(\overline{z})$ is homeomorphic to $(\overline{h})$. If these points, $(\overline{z})$, are the points of the geodesics orthogonal to tangent bundles, (T_z^{q-s-r}), in the multiplicative space $(\Lambda^{q-s} \times T_z^{q-s-r} = 0; r \geq 0)$, then these points are non-singular points, and the cone is a cylinder with all geodesics parallel and have the same lengths. When singularity occurs, the cone concept can be extended into the complex space, by generalizing Lemma 5. This means that the search process for finding non-singular regions within the internal networks continues. In this case, a shrinking criteria is used to explore regions within the dual region (W'_z) for singularity check. Regions, outside of the dual region , can be checked enlarging the cone till all the points on the singularity zone on the dual region (W') in the real space, $(\Re^n)$, are included. Each new cone is then checked for singularities in the internal networks in $(\mathbf{Z}^n)$. Each vertex is the extension of the dual region (W''_z) found by geodesics, (Λ'^{q-s}) that are arbitrary, but similar to the geodesics of the initial dual region $((W''_z \cap \Lambda'^{q-s}))$, with the base of the cone as, $(W'_z \cap \Lambda^{q-s}))$. If the points are non-singular points, the the cone becomes cylinder, with parallel geodesics, with equal lengths.

Hyperplanes in the internal networksin the complex space, $(\mathbf{Z}^n)$, are called geodesics, and are denoted as $(\Lambda^{q-s}; (i-1) \leq q \leq (I); i = 1, \cdots, I-1; s_d = n-k, \cdots, n)$. Geodesics are formulated as $(\Lambda^{q-s} = \frac{\partial^2 \Gamma^{q-s}(\delta(q-s))}{(\partial t)^2} + (\frac{\delta(q-s))}{\eta(\delta(q-s),\delta(q'-s))}^{\alpha,\beta}) \times \frac{\partial \Gamma^{q-s}(\delta(q-s))^{\alpha}}{\partial t} \times \frac{\partial \Gamma^{q-s}(\delta(q-s))^{\beta}}{\partial t})$, where (α) is rotational movement in (3) dimensions, and (β) is movement in dimension not equal to (α), and $(t =\mid \delta(q-s) - \eta(\delta(q-s), \delta(q'-s)) \mid)$. The objective is to show how these geodesics, are used to find the dual segment, $((W'_z \cap \Lambda^{q-s}) \in \mathbf{Z}^n)$, or the vertex of the cone with ordinary points. Ordinary points are those points that are on paths that connect causal elements in $(\mathbf{R}^n)$ that are non-singular. To show this some preliminary ideas should be introduced first. The nodes in the interior networks $(z_{s_d}^{q-s})$ are called Parallax causal elements. Parallax causal elements are those causal element that are not easily identified but are embedded in the structure of a (CRG). Parallax causal elements are closely related to other causal elements, but the connection is hidden. Parallax causal elements are ordinary points when they are in the vertex $(z_{s_d}^{q-s} \in W'_z)$ with base (W') with singular points constituting a singular zone in the dual segment, (W').

If the vertex (W'_z) does not contain ordinary points, then neighborhoods around the vertex are explored. This is done by tracking the geodesics around the vertex. The neighborhoods are either embedded in the vertex or the vertex is a cross-section of the neighborhood. It must be shown that embedded neighborhoods contains points that are homeomorphic to Parallax causal element points. If Parallax causal element points are ordinary points, then all embedded neighboring points are also ordinary points due to homeomorphism effect. The same logic applies if the vertex, (W'_z) is a cross-section of the neighborhood $(B(\xi, \upsilon))$ with the neighboring points, $(\xi_{m_d}^{(q-s)}; m_d = 1, \cdots, M_d)$, and (υ) is the radius of the neighboring zone. Now if Parallax causal elements are not ordinary points, then expanded neighborhoods orthogonal to the geodesics are checked. When Parallax causal elements are not ordinary points, then they are not on the links of the paths in the internal networks, and therefore, are not on the geodesics. These points are ignored. Once a vertex with ordinary points are found then neighboring zones around the vertex are checked for homeomorphism effect. The idea is that if the Parallax causal elements are ordinary points, the paths that include them join causal elements that are stable causal elements and therefore are invariant. The homeomorphism of the neighboring points indicates that these ordinary points are a complete set. Therefore, two types of neighborhoods are considered, one type of neighborhoods are found through shrinking the zones around the vertex, so the zones are embedded zones. The second type of neighboring zones are expansion zones.

Lemma 6. *Given a set of Parallax causal elements, $((z_{s_d}^{q-s}); (i-1) \leq q \leq (I); i = 1, \cdots, I-1; s_d = n-k, \cdots, n)$, where (n) is the total space of possible causal elements, and $(0 \leq s)$, in vertex (W'_z), a neighborhood $(B(\xi, \upsilon))$ of points around each Parallax causal element can be found such that each point,*

$((\xi_{m_d}^{q-s}); (i-1) \leq q \leq (I); i = 1, \cdots, I-1; m_d = 1, \cdots, M_d)$ on $(B(\xi, \upsilon))$, is homeomorphic to each Parallax causal element in the vertex.

Proof. If the vertex, (W_z'), is a fibre bundle vertex resulting from the product of the two spaces of dual hyperplane pencils, $(T_z^{(q-s-r)})$, and geodesics, $(\Lambda^{(q-s)})$, $(T_z^{(q-s-r)} \cap \times \Lambda^{(q-s)})$, then all the points on the boundary of the vertex are at intersections of the tangents with geodesics. If all the points in the product space are on the links of the paths (π_z) in a dense region of the internal networks, then these points are considered to be ordinary points, $(z_{s_d}^{(q-s)})$. Ordinary points are non-singular points in the complex space of internal networks. Any zone embedded in the fibre bundle vertex (W_z'), is a fibre bundle zone, $(B(\xi, \upsilon))$, where the intersection of the links in $(B(\xi, \upsilon))$, and the geodesics, $(\Lambda^{(q-s)})$, are the neighboring points $(\xi_{m_d}^{(q-s)})$. The segment between the ordinary points and the neighboring points are a segment of the geodesics that is equal to (υ), the radius of the orthogonal zone $(B(\xi, \upsilon))$. Since both points, $(\xi_{m_d}^{(q-s)})$, and $(z_{s_d}^{(q-s)})$ are on the geodesics, then the condition for the existence of the geodesics, $((\frac{\delta(q))}{\eta(\delta(q), \delta(q'))}^{\alpha,\beta}) \neq 0)$ is true for both the fibre bundle vertex, and the neighborhood. Therefore all points $(\xi_{m_d}^{(q-s)})$ are homeomorphic to the ordinary points $((z_{s_d}^{(q-s)})$ since the geodesic is considered to be a mapping from (W_z'), to $(B(\xi, \upsilon))$, shown as $(\upsilon = \Lambda^{(q-s)} : W_z' \to (B(\xi, \upsilon))$. □

Lemma 7. *The neighborhood points, $(\xi_{m_d}^{(q-s)})$ of ordinary points, $(z_{s_d}^{(q-s)})$, must be points on the arcs of the paths in the internal networks.*

Lemma 7, is the direct consequence of Lemma 6. Lemma 6, is the generalization of lemma 6, to show that all embedded orthogonal fibre bundle neighboring zones, $((B(\xi, \upsilon))$ consist of neighboring points that are homeomorphic to the ordinary points, $(((z_{s_d}^{q-s}))$, in the vertex, (W_z'). If the ordinary points, exist, then homeomorphic points to these points can be obtained, $(\xi_{m_d}^{(q-s)})$. The homeomorphic points must be on paths that have links with ordinary points as origins and destinations, $((z_{s_d}^{q-s}), (z_{s_d+1}^{q-s}))$.

Proof. Let (λ) be a link with origin an ordinary point $(z_{s_d}^{q-s})$, and destination $(\xi_{m_d}^{(q-s)})$, or inversely, (λ) is a link, with $(\xi_{m_d}^{(q-s)})$, as origin, and $(((z_{s_d+1}^{q-s}))$ as destination. Choose a parameter (t), to represent tracing of the link $(\lambda = \lambda(t))$. Link $(\lambda(t) \times I \to \lambda(t))$, is a link sufficiently close $(I \in [0, 1])$ to links in the vertex, (W_z'), and let $(B(\xi, \lambda(t)) = B(\lambda(t) \times I); I \in [0, 1])$. Let $(\lambda(t) \times \Lambda^{(q-s)} \to \Lambda^{(q-s)}(\lambda(t)))$, geodesics can move along $(\lambda(t))$ links. Let $(T_{\xi,z}^{(q-s-r)}(\lambda(t)) = (B(\xi, \lambda(t)) \times \Lambda^{(q-s)}(\lambda(t)))$, be the tangent line orthogonal to geodesics in fibre bundle neighboring zones, and there exists a mapping $(T_{\xi,z}^{(q-s-r)}(\lambda(t)) \times \Lambda^{(q-s)}(\lambda(t)))$ with following properties:

(1) for $(t = 0)$, $(T_{\xi,z}^{(q-s-r)}(\lambda(0)) \times \Lambda^{(q-s)}(\lambda(0)) \to (z_{s_d}^{(q-s)})$, when the ordinary point is the origin point of link $(\lambda(t))$.
(2) for $(t = 1)$, $(T_{\xi,z}^{(q-s-r)}(\lambda(1)) \times \Lambda^{(q-s)}(\lambda(1)) \to \xi_{m_d}^{(q-s)})$, when the neighboring point is the destination point of link $(\lambda(t))$.

Then $(T_{\xi,z}^{(q-s-r)}(\lambda(t)) \times \Lambda^{(q-s)}(\lambda(t)))$ is the mapping of $(B(\xi, \lambda(t))$ into the vertex (W_z'). Therefore $(B(\xi, \lambda(t)))$ is the homotopy of (W_z').

□

Theorem 6. *Let (π_1) be a homology class of paths that include ordinary points, $(z_{s_d}^{q-s})$, and join causal elements $(x_k^{(i)|_j} \in \Re^n)$, and $(x_{k'}^{(i')|_{j'}} \in \Re^n)$. Then there exists a mapping of any orthogonal fibre bundle containing the homology class paths (π_1), $(B(\xi, \lambda(\pi_1)))$ to any vertex, (W_z'). Thus $(B(\xi, \lambda(\pi_1)))$ is homeomorphic to (W_z'). The causal elements on the extreme ends of homology class of paths (π_1), $(x_k^{(i)|_j})$, and $(x_{k'}^{(i')|_{j'}})$ are non-singular points and are irreducible.*

Proof. Let $(\pi_1 = \pi_1(\lambda(t)))$, where $(\lambda(t))$ is defined as in Lemma 7 be a path containing link $(\lambda(t))$. Let $(\pi_1(\lambda(t)) \times I \to \pi_1(\lambda(t)))$ be a mapping into $([0,1])$ space. $(\pi_1(\lambda(t)))$ is on path (π_z) since link $(\lambda(t))$ is on path (π_z) that connects ordinary points $(z_{s_d}^{(q-s)}, z_{s_d+1}^{(q-s)})$. Let $(T_{\xi,z}^{(q-s-r)}(\pi_1(\lambda(t))) = (B(\xi, \pi_1(\lambda(t))) \times \Lambda^{(q-s)}(\pi_1(\lambda(t))))$, be the tangent line orthogonal to geodesics in fibre bundle neighboring zones, and there exists a mapping $(T_{\xi,z}^{(q-s-r)}\pi_1(\lambda(t))) \times \Lambda^{(q-s)}(\pi_1(\lambda(t)))$ with following properties:

(1) for (t=0), $(T_{\xi,z}^{(q-s-r)}(\pi_1(\lambda(0))) \times \Lambda^{(q-s)}(\pi_1(\lambda(0)) \to ((z_{s_d}^{q-s}))$, when the ordinary point is the origin point of link $(\lambda(t))$.
(2) for (t=1), $(T_{\xi,z}^{(q-s-r)}(\pi_1(\lambda(1))) \times \Lambda^{(q-s)}(\pi_1(\lambda(1)) \to (\xi_{m_d}^{(q-s)}))$, when the neigboring point is the destination point of link $(\lambda(t))$.

Then $(T_{\xi,z}^{(q-s-r)}\pi_1(\lambda(t))) \times \Lambda^{(q-s)}(\pi_1(\lambda(t)))$ is the mapping of $(B(\xi, \pi_1(\lambda(t)))$ into the vertex (W_z'). Therefore $(B(\xi, \pi_1(\lambda(t))))$ is the homotopy of (W_z').

□

Corollary 1. *There exists a chain of homeomorphic orthogonal fibre bundle zones, $(B_g(\xi, \upsilon_g))$ to the vertex, (W_z').*

The proof of Corollary 1 is the extension of Theorem 6 and Lemmas 6, and 7. The outline of the proof is as follows: Let $(\lambda_g(t^*))$, be defined as links on class (π_1) paths such that $(\xi_{m_d}^{(q-s)})$, is either the origin of the link or the destination of the link. (t^*) is a a parameter on the second copy of (I). Let $(\lambda_g(t^*) \times I \times I \to \lambda_g(t^*))$, be defined as a homeomorphism into the second copy of (I). Let $(\pi_1(\lambda_g(t*)))$ be defined as in Theorem 6, as a homeomorphism of path $(\pi_1(\lambda_g(t^*)))$ onto the second copy of (I). By Theorem 6, and Lemmas 6, any orthogonal fibre bundle, $(B_g(\xi, \upsilon_g))$ is homeomorphic to the vertex (W_z').

Singularities in the internal networks occur when a geodesic does not intersect any links containing ordinary nodes, $(z_{s_d}^{(q-s)})$, in the internal networks, and thus makes it impossible to perceive a vertex (W_z'). In this case, must restart the search procedure from the beginning by going back to a face on the rectangular slab that is different from the one that was checked initially, $(V^{p'} \neq V^p)$. The search process restart by cutting a segment (W) using hyperplanes, $(L^{(i)})$, and hyperplane pencils, $(\Gamma^{(i)})$. Then proceed with finding the dual of (W), (W') and its' corresponding dual hyperplanes, $(L'^{(i)})$, and dual hyperplane pencils, $(\Gamma'^{(i)})$. If dual hyperplane pencils, exist for all points on the dual segment, (W'), then all point on the segment (W), are non-singular points, and therefore, the causal elements linked by arcs on paths inside the cut segment, (W), are stable, irreducible, causal elements, and any sub-group of (CRG) is a complete sub-group that is optimal. If on the other hand dual hyperplane pencils, do not exist for all points on the dual segment, (W'), then within the singularity zone, an arbitrary dual hyperplane pencil, $(\Gamma_*^{(q-s)})$ extended to the internal networks in $(\mathbf{Z}^n)$. At this point the arbitrary dual hyperplane pencil transforms into a geodesic $(\Lambda^{(q-s)})$. If geodesics hit links in the internal networks that contain ordinary points otherwise known as Parallax causal elements, then it is possible to designate a dual zone, (W_z'), that is considered to be the vertex, of a cone with base the singular zone of the dual segment, (W'). If all points (W_z') are on links, and the geodesics are orthogonal to tangent bundles at these points, then it is considered that the causal elements linked through the paths containing these links in the dual segment (W'), are stable, and irreducible causal elements, and any sub-group consisting of these causal elements is optimal. If geodesics do not hit links in the internal networks, then the search process restarts.

4 Conclusion

In this paper a search technique for finding stable and complete sub-groups of (CRG) is proposed using a new homology approach. The objective of this new approach is to find the equilibrium state of (CRG) by finding optimal stable, irreducible, and complete sub-groups. An equilibrium state is indicative of an optimal

(CRG). It is assumed that at equilibrium a (CRG) is stable (predictable), and thus does not demonstrate randomness behavior. The main element of this type of random algebraic groups is causality. What causes instability is the occurrence of singularities. Singularities are directly related to causality. Causality is detailed as is shown in Figure 12.

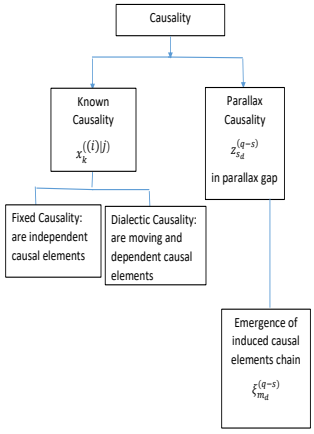

Figure 13. Causality

As is shown in Figure 13, there are two types of causalities: 1) known causality, $(x_k^{(i)|_j})$, 2) Parallax causality, $(z^(q-s)_{s_d})$. Known causal elements are either fixed which means that causal elements are independent and they are linked through fixed paths that contain fixed intermediate causal chains. Dialectic causal elements are dependent and posses internal triggering elements of change inside the causal elements. For example, each dialectic causal element possesses several dimensions or characteristics, and each dimension possesses several degrees of intensities. Dialectic causal elements are linked through different paths that contain variable intermediate causal chains, that lead to the formation of networks that consist alternative paths. Optimal sub-groups are found on alternative paths. In the case of singularity, causal elements become Parallax causal elements in complex space. The behavior of Parallax causal elements in complex space is similar to the behavior of causal elements in real space which leads to the formation of networks and paths. The internal networks is a Parallax gap. This is the physical distance between the causal elements, and related causal elements that initially do not seem to be related to causal elements. Search for regions of non-singularity in the complex space ends in finding those causal elements that are stable, and complete. Hyperplanes and hyperplane pencils are used in the search, in real space, and geodesics are used in complex space. Geometrical representation has been used for algebraic groups, but is a novel approach for (CRG). (CRG) is represented as a rectangular slab. A rectangular slab has eight faces or sides. The space between every two faces of the rectangular slab is called a Parallax gap in complex space. The network in Parallax gap is called an internal networks. On each face of the rectangular slab, there exists a network consisting of links and paths that join each causal point of the rectangular slab. Each point represents a causal element. The main tools used are hyperplanes and hyperplane pencils to cut or isolate segments of the network on a face of rectangular slab, and dual hyperplanes and dual hyperplane pencils are used to find dual regions. In the internal network, hyperplane pencils are transformed into geodesics. If dual regions exist in the real space, for a set of causal elements and each point on the dual region is a point on dual hyperplane pencils that is orthogonal to fibre bundles that pass through these points, then it is assumed that these points are non-singular, otherwise if for some points on the dual region there exists no multiplicative space of hyperplane pencils and fibre bundles, then singularity occurs. In the case of singularity, search for dual regions continues in complex space using geodesics. Non-singularity of points on dual regions occur if these points are in a multiplicative space where geodesics are orthogonal to tangent fibre bundles. These non-singular points indicate that causal elements are stable, irreducible, and any sub-group of (CRG) that includes these causal elements is complete and thus optimal. If non-singularity occurs, then the search for non-singular points continues. The search for optimal sub-groups of (CRG) is outlined in Figure 14.

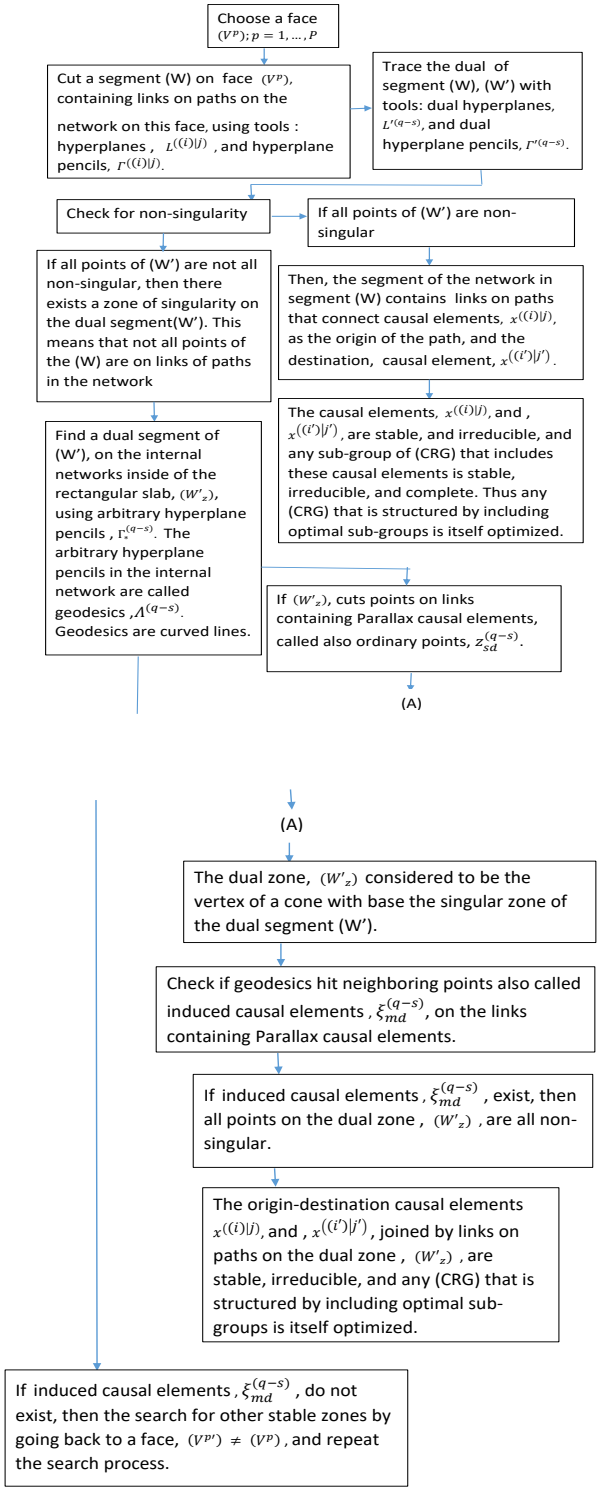

Figure 14. Singularity search process

5 Notation

(CRG) = Causal Random Groups.
$(\Re^n)$ = Real space.
$(\mathbf{Z}^n)$ = Complex space.
$(G(X); X \subset \Re^n)$ = Causal Random Group, (CRG)
$(X = \{x^k_{i,j}, k = 1, 2, , \cdots, K; i = 1, \cdots, I; j = 1, \cdots, J\})$ = Space of causal elements
$(k = 1, 2, , \cdots, K)$ = Number of causal elements with maximum number, $(K \leq n)$ less than or equal to (n), where (n) is the number of causal elements in space (X).
$(i = 1, \cdots, I)$ = Number of dimensions for each causal element with the maximum number of dimensions equal to (I).
**(I) also used inside proofs to represent an identity space.
$(j = 1, \cdots, J)$ = Levels of intensities of each dimension. (J) is the maximum levels of intensities.
$(x^{(i)|_j}_k; k \leq K)$ = Each element of space (X).
$(G(X, V^p); p = 1, \cdots, P)$ = A (CRG) with geometrical representation.
(p) = Face number.
(V) = A face.
(P) = Maximum number of possible face numbers.
$(y^{(i)|_j}_{c_a}; c_a = 1, \cdots, C_a)$ = Chain causal elements.
(C_a) = Maximum number of causal chain points.
$(\pi(y^{(i,i')|_{j,j'}}_{c_a}, y^{(i,i')|_{j,j'}}_{c_a+1}); c_a); \leq K - 1; y^{(i,i')|_{j,j'}}_1 = x^{(i)|_j}_k, y^{(i,i')|_{j,j'}}_{C_a} = x^{(i')|_{j'}}_{k'}; i \neq i'; j \neq j'; k \neq k';)$ = Paths on face (V^p) in $(\Re^n)$.
$(\delta((i)\,|_j) = (|\, j \,|_i \times \nu_{j|_i}))$ = Gravitational force of dimensions (i) in real space.
$(|\, j \,|_i; j = 1, \cdots, J; \forall(i))$ = Magnitude of intensity of dimension (i).
$(\nu_{j|_i}; j = 1, \cdots, J; \forall(i)),$ = Velocity of interaction among (j) intensities of dimension (i).
$(\eta(\delta(q-s), \delta(q'-s)); (i-1) \geq q \leq I; i = 1, \cdots, I-1)$ = Covariance of gravitational forces of dimensions $(q-s)$, and $(q'-s)$.
$(\tau(j)\,|_i)$ = Intensity level causality forces.
$(z^{q-s}_{s_d}); s_d = n-k, \cdots, n)$ = Parallax causal points in the internal networks in $(\mathbf{Z}^n)$.
$(\xi^(q-s)_{m_d}; m_d = 1, \cdots, M_d)$ = Neighboring points, also called induced causal elements.
(M_d)= is the number of induced causal elements in the causal chain.
$(\pi_z \in \mathbf{Z}^n)$ = Paths in internal networks.
$(\delta(q-s))$ = Gravitational force in complex space.
$(\eta(\delta(q-s), \delta(q'-s))$ = Covariances among parallax causal nodes.
$(L^{(i)})$ = Hyperplanes in $(\Re^n)$.
$(L'^{(i)})$ = Dual hyperplane in $(\Re^n)$.
$(\Gamma^{(i)})$ = Hyperplane pencils in $(\Re^n)$.
$(\Gamma'^{(i)})$ = Dual Hyperplane pencils in $(\Re^n)$.
$(\Lambda^{(q-s)})$ = Geodesics in the complex space, $(\mathbf{Z}^n)$.
(W'_z) = Dual projection of a singular zone in the internal network in $(\mathbf{Z}^n)$, in the dual region (W').
$((B(\xi, \upsilon))$ = Orthogonal fibre bundle.
$(T^{(q-s)})$ = Tangent fibre bundles on $(\beta(W))$ in $(\Re^n)$.
$(T^{(q-s-r)})$ = Tangent fibre bundles on $(W'))$ in $(\Re^n)$.
$(T^{(q-s-r)}_z)$ = Tangent fibre bundles on $(W'_z))$ in $(\mathbf{Z}^n)$.
$(T^{(q-s-r)}_{\xi,z})$ = Tangent fibre bundles on $((B(\xi, \upsilon))$ in $(\mathbf{Z}^n)$.

References

[1] A. W. Wallace, *Homology Theory on Algebraic Varieties*, Dover Publication Inc. (1958).

[2] A. Weil, *Sur la théorie des formes différentielles attachées à une variéte analytique complexe*, Comm. Math. Helv. vol. 20,(1947), 110-116.

[3] N. E. Steenrod, *The topology of fibre bundles*, Princeton (1951).

[4] R. Bala, B. Ram, *Trigonometric series with semi-convex coefficients*, Tamang J. Math. 18, 1 (1987), 75-84.

[5] B. Ram, *Convergence of certain cosine sums in the metric space L*, Proc. Amer. Math. Soc. 66 (1977), 258-260.

[6] H. Henning, *Die Qualitätenriehe des Geschmacks*, Zeitschrift für psychologie und Physiologie der Sinnesorgane, 74: 203-219 (1916).

[7] W. T. Maddox, *Perceptual and decisional separability*, In Ashby, F.G. ed. Multidimensional Models of Perception and Cognition, Hillsdale, NJ: 147-180 (1992).

[8] A. Clark, *Sensory qualities*, Clarendon Press, Oxford, (1993).

[9] N.K. Sedov, *Trigonometric Series and Their Applications* (in Russian), Fizmatgiz, Moscow 1961.

[10] S. Zizek, *The Parallax View*, The MIT Press, Cambridge, Massachusetts, (2006).